A NOTE ABOUT THE GEOMETRIC OPTIMAL CONTROL OF THE COPEPOD SWIMMER

BERNARD BONNARD, MONIQUE CHYBA, JÉRÉMY ROUOT, DAISUKE TAKAGI, RONG ZOU

Bernard Bonnard

Inria Sophia Antipolis et Institut de Mathématiques de Bourgogne
9 avenue Savary
21078 Dijon, France

Monique Chyba, Daisuke Takagi

2565 McCarthy the Mall
Department of Mathematics
University of Hawaii
Honolulu, HI 96822, USA

Jérémy Rouot

Inria Sophia Antipolis
2004 route des lucioles
06902 Sophia Antipolis, France

Rong Zou

Department of Systems Innovation,
Graduate School of Engineering Science
Osaka, Japan

Abstract. The objective of this note is to made preliminary remarks concerning the optimal locomotion of the Copepod swimmer described by a simple model concerning swimming at low Reynolds number, in the framework of Sub-Riemannian geometry. In particular the role of both normal and abnormal geodesics is related to observed geometric motions.

1. **Introduction.** Models concerning the swimming of micro-organisms were introduced in the fifties, see for example [11],[14] and can be easily observed. Assuming that the locomotion is performed minimizing the expended mechanical power they were analyzed in several articles in the framework of variational analysis or optimal control [1],[3],[13],[4],[6].

The fundamental model is the so-called three-links Purcell swimmer which consists into three rigid links representing respectively the leg, the body and the arm. The configuration of the swimmer is described by two angles $\theta = (\theta_1, \theta_2)$ with three

2010 *Mathematics Subject Classification.* 58F15, 49K15, 93C10, 70Q05.

Key words and phrases. Purcell swimmer, SR-geometry, periodic optimal control.

The third author is supported by the French Space Agency CNES, R&T action R-S13/BS-005-012 and by the région Provence-Alpes-Côte d'Azur.

other variables $q = (x, y, \Phi)$ describing respectively the position and the orientation of the body. The system can be written as

$$\dot{q} = D(\Phi)G(\theta)\dot{\theta}$$
$$\dot{\theta} = H(\theta)\tau$$

and $D(\Phi)$ is the rotation matrix

$$D(\Phi) = \begin{pmatrix} \cos(\Phi) & -\sin(\Phi) & 0 \\ \sin(\Phi) & \cos(\Phi) & 0 \\ 0 & 0 & 1 \end{pmatrix}$$

By denoting $u = \dot{\theta}$, the mechanical power is

$$\tau u = uH^{-1}u$$

and the energy minimization problem becomes

$$\int_0^T (uH^{-1}u)dt$$

where u is taken as the control variable, see [10] for a complete description of the matrices G and H.

This control problem falls into the Sub-Riemannian (SR) framework, it is complex even locally and is related to the Cartan flat SR-model [4]. However, the simplest SR-case called the Heisenberg case provides us already with some information. The Heisenberg control system is given by

$$\dot{x} = u_1\theta_2 - u_2\theta_1$$
$$\dot{\theta}_1 = u_1, \quad \dot{\theta}_2 = u_2$$

while minimizing the integral

$$\int_0^T (u_1^2 + u_2^2)dt.$$

A simple integration of the non planar geodesics starting from the origin gives

$$\theta_1(t) = \frac{A}{\lambda}\left(\sin(\lambda t + \varphi) - \sin(\varphi)\right)$$
$$\theta_2(t) = \frac{A}{\lambda}\left(\cos(\lambda t + \varphi) - \cos(\varphi)\right)$$
$$x(t) = \frac{A^2}{\lambda}t - \frac{A^2}{\lambda^2}\sin(\lambda t)$$

where A, λ and φ are parameters related to the initial velocity. Both angular variables are periodic motion corresponding to strokes to provide the displacement $x(2\pi/\lambda)$, whose average is given by A^2/λ^2, the period of the stroke being $2\pi/\lambda$. A standard computation of conjugate points shows that such geodesic is optimal up to $t = 2\pi/\lambda$ (included). In this example the optimal displacement corresponds to a simple stroke using the conjugate test and the cut locus computation given by the axis Ox.

While this model can provide some insights on optimal locomotion, it is too primitive because:

1. The geodesic flow is integrable due to a symmetry of revolution along Ox and every $\theta-$motion is periodic.

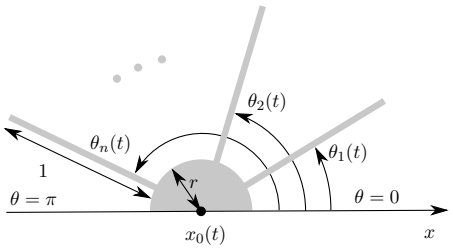


FIGURE 1. Sketch of the upper half of a symmetric swimmer.

2. The model is quasi-homogeneous , θ_1 and θ_2 are of weight 1 and x is of weight 2, and invariant in the Heisenberg group.

A physical model describing the locomotion of copepods (an abundant form of zooplankton) proposed in [12] consists in two pairs of symmetric legs with respective angles θ_1, θ_2 with respect to the displacement direction Ox (Fig.1:n links).
The swimming velocity at x_0 is given by

$$\dot{x}_0 = \frac{\dot{\theta}_1 \sin(\theta_1) + \dot{\theta}_2 \sin(\theta_2)}{2 + \sin^2(\theta_1) + \sin^2(\theta_2)}$$

and the controls are the angular velocities

$$\dot{\theta}_1 = u_1, \quad \dot{\theta}_2 = u_2.$$

We have state constraints $\theta_i \in [0, \pi],\ i = 1, 2,\ \theta_2 \leq \theta_1$.
A simplified cost can be identified to

$$\int_0^T (u_1^2 + u_2^2) dt$$

but the true cost corresponding to the mechanical energy of the system is given by the quadratic form

$$\dot{q}^t M \dot{q}$$

where $q = (x_0, \theta_1, \theta_2)$, M is the symmetric matrix

$$M = \begin{pmatrix} 2 - 1/2(\cos^2(\theta_1) + \cos^2(\theta_2)) & -1/2\sin(\theta_1) & -1/2\sin(\theta_2) \\ -1/2\sin(\theta_1) & 1/3 & 0 \\ -1/2\sin(\theta_2) & 0 & 1/3 \end{pmatrix}. \qquad (1)$$

The interest to study this model is double. First, it describes accurately the motion of a micro-swimmer which can be easily observed experimentally. This will be the basis of the description of two types of strokes. Second, it is a global model of SR-geometry which can be analyzed in details, showing in particular the role of normal and abnormal geodesics in the motion, in accordance with the observations. See also [2] for a similar model but a different analysis in which second order optimality conditions are not used.

This note is organized in two sections. In section 2, we recall the results of observations concerning the copepod swimmer [12] and the mathematical tools from geometric optimal control (see [5] for a general reference). The section 3 contains the contribution of this note based on a geometric analysis and numerical simulations to describe the optimal strokes and confirming the observations.

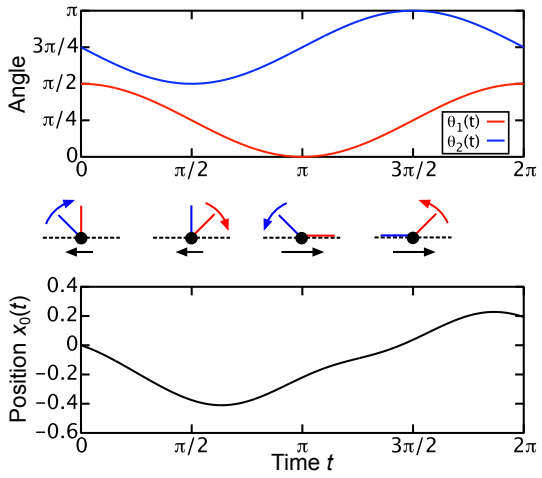


FIGURE 2. Two legs oscillating sinusoidally according to $\theta_1 = \pi/4 + a\cos t$ and $\theta_2 = 3\pi/4 + a\cos(t+\pi/2)$, where $a = \pi/4$ is the amplitude. The second leg (blue) oscillates about $\Phi_2 = 3\pi/4$, while the first leg (red) oscillates about $\Phi_1 = \pi/4$ with a phase lag of $\pi/2$. Arrows show the swimmer and leg velocities at four representative stages of the cycle. The swimmer position x_0 translates about a fifth of the leg length after one cycle.

2. Preliminary results.

2.1. Geometric analysis of a copepod swimmer.

A (general) stroke is a periodic motion of the angular variables θ_1, θ_2 where the period can be fixed to 2π and to produce a displacement $x_0(2\pi) - x_0(0)$ of the swimmer.

In [12], two types of geometric motions are described:

First case: (Fig.2) The two legs are assumed to oscillate sinusoidally according to

$$\theta_1 = \Phi_1 + a\cos(t), \quad \theta_2 = \Phi_2 + a\cos(t + k_2)$$

with $a = \pi/4$, $\Phi_1 = \pi/4$, $\Phi_2 = 3\pi/4$ and $k_2 = \pi/2$. This produces a displacement $x_0(2\pi) = 0.2$.

Second case: (Fig.3) The two legs are paddling in sequence followed by a recovery stroke performed in unison. In this case the controls $u_1 = \dot\theta_1$, $u_2 = \dot\theta_2$ produce bang arcs to steer the angles between from the boundary 0 of the domain to the boundary π, while the unison sequence corresponds to a displacement from π to 0 with the constraint $\theta_1 = \theta_2$.

Our main objective is to relate these properties to geometric optimal control.

2.2. Abnormal curves in the copepod swimmer.

We introduce $q = (x_0, \theta_1, \theta_2)$, then the system is written as a driftless affine control

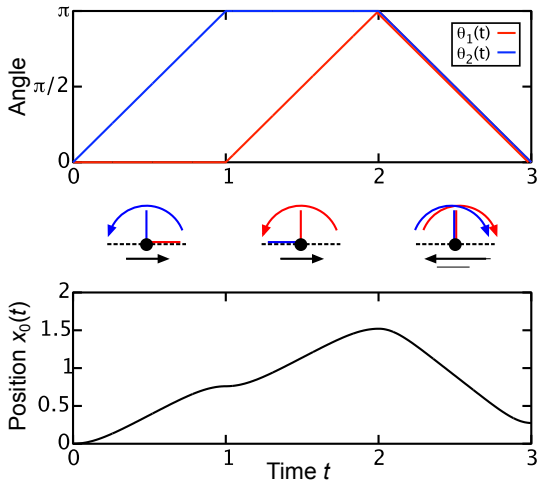


FIGURE 3. Two legs paddling in sequence. The legs perform power strokes in sequence and then a recovery stroke in unison, each stroke sweeping an angle π. Arrows show the swimmer and leg velocities at three representative stages of the cycle.

system

$$\dot{q}(t) = \sum_{i=1}^{2} u_i(t) F_i(q(t))$$

where the control vector fields are given by

$$F_i = \frac{\sin(\theta_i)}{\Delta} \frac{\partial}{\partial x_0} + \frac{\partial}{\partial \theta_i}$$

with $\Delta = 2 + \sin^2(\theta_1) + \sin^2(\theta_2)$. We denote by D the distribution $span\{F_1, F_2\}$.

The Lie bracket of two vector fields F, G is computed with the convention

$$[F, G](q) = \frac{\partial F}{\partial q}(q) G(q) - \frac{\partial G}{\partial q}(q) F(q).$$

Finally, we denote by $p = (p_1, p_2, p_3)$ the adjoint vector associated with q.

We first recall a basic fact concerning the local classification of two-dimensional distributions, in relation with abnormal curves.

2.2.1. *Local classification of two-dimensional distributions in dimension three and abnormal curves.*
Let $D = span\{G_1, G_2\}$ be the distribution generated by two vectors fields G_1, G_2 in $\mathbb{R}^3$. Let $z = (q, p)$ and denote $H_i(z) = \langle p, G_i(q) \rangle$, $i = 1, 2$ the Hamiltonian lifts. The Poisson bracket is given by

$$\{H_1, H_2\}(z) = dH_1(\vec{H}_2)(z) = \langle p, [G_1, G_2](q) \rangle.$$

Abnormal curves are defined by

$$H_1(z) = H_2(z) = 0$$

and differentiating using the dynamics

$$\frac{dz}{dt} = \sum_{i=1}^{2} u_i H_i(z)$$

one gets the relations

$$\begin{aligned} &\{H_1, H_2\}(z) = 0 \\ &u_1 \{\{H_1, H_2\}, H_1\}(z) + u_2 \{\{H_1, H_2\}, H_2\}(z) = 0 \end{aligned}$$

defining the corresponding controls.

There are tools from singularity theory to classify the distributions, see [15] and we present only the two (stable) models related to our study.

Contact case. We say that q_0 is a *contact point* if $\{G_1, G_2, [G_1, G_2]\}$ is of dimension 3 at q_0. At such a point identified to 0, there exists local coordinates $q = (x, y, z)$ such that

$$D = ker(\alpha), \qquad \alpha = ydx + dz.$$

Observe $d\alpha = dy \wedge dx$ (Darboux form) and $\frac{\partial}{\partial z}$ is the characteristic direction of $d\alpha$. This form is equivalent to

$$D = ker(\alpha'), \qquad \alpha' = dz + (xdy - ydx).$$

with

$$\begin{aligned} &D = span\{G_1, G_2\}, \qquad && G_1 = \frac{\partial}{\partial x} + y\frac{\partial}{\partial z}, \\ &G_2 = \frac{\partial}{\partial y} - x\frac{\partial}{\partial z}, && G_3 = [G_1, G_2] = \frac{\partial}{\partial z}. \end{aligned} \tag{2}$$

The Martinet case. A point q_0 is a *Martinet point* if at q_0, $[G_1, G_2] \in span\{G_1 G_2\}$ and at least one Lie bracket $[[G_1, G_2], G_1]$ or $[[G_1, G_2], G_2]$ does not belong to D. Then there exists local coordinates $q = (x, y, z)$ near q_0 identified to 0 such that

$$D = ker\omega, \qquad \omega = dz - \frac{y^2}{2}dx$$

where

$$\begin{aligned} &G_1 = \frac{\partial}{\partial x} + \frac{y^2}{2}\frac{\partial}{\partial z}, \quad G_2 = \frac{\partial}{\partial z}, \quad G_3 = [G_1, G_2] = y\frac{\partial}{\partial z} \\ &[[G_1, G_2], G_1] = 0, \quad [[G_1, G_2], G_2] = \frac{\partial}{\partial z}. \end{aligned} \tag{3}$$

The surface $\Sigma : y = 0$ is called the *Martinet surface* and is foliated by abnormal curves, solutions of $\frac{\partial}{\partial z}$. In particular through 0 it corresponds to the curve $t \to (t, 0, 0)$.

Remark 1. One more generic situation is the so-called tangential case, which will be not needed in our analysis.

2.2.2. *Computations in the copepod case.*
We have

$$F_3 = [F_1, F_2] = f(\theta_1, \theta_2)\frac{\partial}{\partial x_0}$$

with

$$f(\theta_1,\theta_2)=\frac{2\sin(\theta_1)\sin(\theta_2)(\cos(\theta_1)-\cos(\theta_2))}{\Delta^2},$$
$$[[F_1,F_2],F_1]=\frac{\partial f}{\partial\theta_1}(\theta_1,\theta_2)\frac{\partial}{\partial x_0},\qquad [[F_1,F_2],F_2]=\frac{\partial f}{\partial\theta_2}(\theta_1,\theta_2)\frac{\partial}{\partial x_0}.$$

In particular we deduce the following lemma.

Lemma 2.1. *The singular set* $\Sigma:\{q;\ \det(F_1(q),F_2(q),[F_1,F_2](q))=0\}$, *where the vector fields* $F_1,F_2,[F_1,F_2]$ *are collinear, is given by* $2\sin(\theta_1)\sin(\theta_2)(\cos(\theta_1)-\cos(\theta_2))=0$ *that is*

- $\theta_1=0$ *or* π,
- $\theta_2=0$ *or* π,
- $\theta_1=\theta_2$.

and formed the boundary of the physical domain: $\theta_i\in[0,\pi],\theta_1\leq\theta_2$, *with respective controls* $u_1=0,\ u_2=0$ *or* $u_1=u_2$.

Remark 2. This gives the interpretation of the policy in Fig.3.

To analyse the first situation of Fig.2, the mechanical energy has to be used in relation with SR-geometry.

2.3. **SR-geometry.**

The problem is written

$$\dot q=\sum_{i=1}^{2}u_iG_i(q),\quad \text{Min}\to\int_0^T(u_1^2+u_2^2)dt,$$

where the cost is for fixed T and corresponds to the energy. In our case we use the normalized value $T=2\pi$.

In this representation, we assume that the vector fields G_1,G_2 are orthonormal.

According to Pontryagin maximum principle, we introduce the pseudo-Hamiltonian in the normal case

$$H(z,u)=\sum_{i=1}^{2}u_iH_i-\frac12\sum_{i=1}^{2}u_i^2,$$

where H_i are the Hamiltonian lifts $\langle p,G_i(q)\rangle$. The maximization condition gives us $\frac{\partial H}{\partial u_i}=0$. Hence $u_i=H_i$ and plugging such u_i into H gives the Hamiltonian in the normal case

$$H_n=\frac12\left(H_1^2+H_2^2\right).$$

In the contact case, it corresponds to the Heisenberg case while in the Martinet case, it corresponds to the flat Martinet case. In both cases it amounts to impose that G_1,G_2 are orthonormal and the associated distribution is nilpotent.

Definition 2.2. A normal stroke is a solution of H_n such that θ_1 and θ_2 are periodic with period 2π.

According to the transversality conditions of the maximum principle the dual variables p_2 and p_3 are such that p_2 and p_3 are both periodic of period 2π (to produce a smooth solution).

Second order optimality condition. In the normal case, the *first conjugate point* corresponds to the first point where a normal geodesic ceases to be minimizing which

respect to the C^1-topology on the set of curves and they can be computed using the Hampath code [7].

This leads to the following definition.

Definition 2.3. A normal stroke is called optimal on $[0, 2\pi]$ if there exists no conjugate point on the interval $]0, 2\pi]$.

3. Computations and analysis in the copepod swimmer.

3.1. Simplified cost.

First of all we consider the simplified cost

$$\text{Min} \rightarrow \int_0^T (u_1^2 + u_2^2) dt$$

in relation with the contact case.

Outside the singular set Σ, we have only contact points. Introducing the Hamiltonian lifts: $H_i = \langle p, F_i(q) \rangle$ for $i = 1, 2$, $H_3 = \langle p, [F_1, F_2](q) \rangle$, the set $\{q, H_1, H_2, H_3\}$ are coordinates and

$$\begin{aligned} H_1 &= \frac{p_1 \sin\theta_1}{\Delta} + p_2, \qquad H_2 = \frac{p_1 \sin\theta_2}{\Delta} + p_3, \\ H_3 &= \frac{2p_1 \sin\theta_1 \sin\theta_2 (\cos\theta_1 - \cos\theta_2)}{\Delta^2}. \end{aligned} \tag{4}$$

Moreover the problem is isoperimetric that is: $\dot{p}_1 = 0$.
Computing one gets

$$\begin{aligned} \dot{H}_1 = dH_1(\vec{H}_n) = dH_1 \left(\frac{1}{2} \overrightarrow{(H_1^2 + H_2^2)} \right) = \{H_1, H_2\} H_2, \\ \dot{H}_2 = dH_2(\vec{H}_n) = dH_1 \left(\frac{1}{2} \overrightarrow{(H_1^2 + H_2^2)} \right) = \{H_2, H_1\} H_1. \end{aligned}$$

Hence

$$\dot{H}_1 = H_2 H_3, \qquad \dot{H}_2 = -H_1 H_3.$$

Moreover

$$\dot{H}_3 = dH_3(\vec{H}_n) = dH_3(\frac{1}{2} \overrightarrow{(H_1^2 + H_2^2)}) = \{H_3, H_1\} H_1 + \{H_3, H_2\} H_2$$

with

$$\{H_3, H_1\}(z) = \langle p, [[F_1, F_2], F_1](q) \rangle, \quad \{H_3, H_2\}(z) = \langle p, [[F_1, F_2], F_2](q) \rangle.$$

At a contact point $\{F_1, F_2, F_3\}$ forms a frame, hence

$$[[F_1, F_2], F_1](q) = \sum_{i=1}^{3} \lambda_i(q) F_i(q)$$

and computing one gets,

$$\lambda_1 = \lambda_2 = 0, \qquad \frac{\partial f}{\partial \theta_1} = \lambda_3 f.$$

Similarly,

$$[[F_1, F_2], F_2](q) = \sum_{i=1}^{3} \lambda_i'(q) F_i(q),$$

and

$$\lambda_1' = \lambda_2' = 0, \qquad \frac{\partial f}{\partial \theta_2} = \lambda_3' f.$$

We conclude that

$$\begin{aligned} &\dot{H}_1 = H_2 H_3, \quad \dot{H}_2 = -H_1 H_3, \\ &\dot{H}_3 = H_3 \left(\lambda_3 H_1 + \lambda_3' H_2\right). \end{aligned} \tag{5}$$

We introduce a new time reparametrization with $ds = H_3 dt$ and we obtain

$$\frac{dH_1}{ds} = H_2, \qquad \frac{dH_2}{ds} = -H_1, \qquad \frac{dH_3}{ds} = \lambda_3 H_1 + \lambda_3' H_2.$$

Hence we have the harmonic oscillator since $H_1'' + H_1 = 0$ when differentiating with respect to the new time s.

Furthermore H_3 can be computed using the remaining equation (5). Observe that with the approximation λ_3, λ_3' constant, the equation is

$$\frac{dH_3}{ds} = A\cos(s+\rho).$$

In this formalism, the Heisenberg case is when $\lambda_3 = \lambda_3' = 0$.

3.2. **True Cost.**

In this case the computation is more intricated since F_1, F_2 are not orthonormal. The energy associated with the mechanical energy matrix M defined by (1) is given using optimal control formalism by

$$a(q)u_1^2 + 2b(q)u_1u_2 + c(q)u_2^2,$$

where

$$\begin{aligned} a &= \frac{1}{3} - \frac{\sin^2\theta_1}{2(2+\sin^2\theta_1+\sin^2\theta_2)}, \\ b &= -\frac{\sin\theta_1\sin\theta_2}{2(2+\sin^2\theta_1+\sin^2\theta_2)}, \\ c &= \frac{1}{3} - \frac{\sin^2\theta_2}{2(2+\sin^2\theta_1+\sin^2\theta_2)}. \end{aligned}$$

with

$$\dot{\theta}_1 = u_1, \qquad \dot{\theta}_2 = u_2.$$

The pseudo-Hamiltonian in the normal case is

$$H(q,p) = u_1 H_1(q,p) + u_2 H_2(q,p) - \frac{1}{2}\Big(a(q)u_1^2 + 2b(q)u_1u_2 + c(q)u_2^2\Big).$$

and the normal controls are computed solving the equations

$$\frac{\partial H}{\partial u_1} = 0, \qquad \frac{\partial H}{\partial u_2} = 0.$$

Computing one gets

$$\begin{aligned} u_1 &= -\frac{3(4H_1 + 2H_1\sin^2\theta_1 + 3H_2\sin\theta_1\sin\theta_2 - H_1\sin^2\theta_2)}{\sin^2\theta_1+\sin^2\theta_2-4}, \\ u_2 &= -\frac{9H_1\sin\theta_1\sin\theta_2 + 6H_2(2+\sin^2\theta_2) - 3H_2\sin^2\theta_1}{\sin^2\theta_1+\sin^2\theta_2-4}. \end{aligned}$$

Plugging such u into the pseudo-Hamiltonian gives the true Hamiltonian

$$
\begin{aligned}
H_n &= u_1 H_1 + u_2 H_2 - \frac{1}{2}\Big(a(q)u_1^2 + 2b(q)u_1u_2 + c(q)u_2^2\Big) \\
&= -\frac{3}{2(\sin^2\theta_1+\sin^2\theta_2-4)(\sin^2\theta_1+\sin^2\theta_2+2)}\Big(2\big(\sin^2\theta_1+\sin^2\theta_2\big){p_1}^2 \\
&\quad + \big(2\sin^4\theta_1+\sin^2\theta_1\sin^2\theta_2-\sin^4\theta_2+8\sin^2\theta_1+2\sin^2\theta_2+8\big){p_2}^2 \\
&\quad + \big(-\sin^4\theta_1+\sin^2\theta_1\sin^2\theta_2+2\sin^4\theta_2+2\sin^2\theta_1+8\sin^2\theta_2+8\big){p_3}^2 \\
&\quad + \big(4\sin^3\theta_1+4\sin^2\theta_2\sin\theta_1+8\sin\theta_1\big)p_1\,p_2 \\
&\quad + \big(4\sin^2\theta_1\sin\theta_2+4\sin^3\theta_2+8\sin\theta_2\big)p_1\,p_3 \\
&\quad + \big(6\sin\theta_2\sin^3\theta_1+6\sin^3\theta_2\sin\theta_1+12\sin\theta_1\sin\theta_2\big)p_2\,p_3\Big)
\end{aligned}
\tag{6}
$$

and leads to the dynamics in the (q,p) coordinates

$$
\begin{aligned}
\dot{x}_0 &= \frac{\partial H_n}{\partial p_1} = -\frac{(\sin^2\theta_1+\sin^2\theta_2)p_1+(\sin^3\theta_1+(2+\sin^2\theta_2)\sin\theta_1)p_2+(\sin^2\theta_1\sin\theta_2+\sin\theta_2(2+\sin^2\theta_2))p_3}{\big(\cos(2\theta_1)+\cos(2\theta_2)-6\big)\big(\cos(2\theta_1)+\cos(2\theta_2)+6\big)} \\
\dot{\theta}_1 &= \frac{\partial H_n}{\partial p_2} = -\frac{3(4\sin\theta_1 p_1+(8-2\sin^2\theta_2+4\sin^2\theta_1)p_2+6\sin\theta_1\sin\theta_2 p_3)}{2(\sin^2\theta_1+\sin^2\theta_2-4)} \\
\dot{\theta}_2 &= \frac{\partial H_n}{\partial p_3} = -\frac{3(2\sin\theta_2 p_1+3\sin\theta_1\sin\theta_2 p_2+(4-\sin^2\theta_1+2\sin^2\theta_2)p_3)}{2(\sin^2\theta_1+\sin^2\theta_2-4)}.
\end{aligned}
$$

$$
\begin{aligned}
\dot{p_1} &= -\frac{\partial H_n}{\partial x_0} = 0. \\
\dot{p_2} &= -\frac{\partial H_n}{\partial \theta_1} \\
&= -\frac{6\cos\theta_1}{\left(\cos(2\theta_2)+\cos(2\theta_1)-6\right)^2\left(\cos(2\theta_2)+\cos(2\theta_1)+6\right)^2}\Big(2p_3\left(\cos(2\theta_1)-5\right)\sin^3\theta_2\Big(3p_2\cos(2\theta_1)-39p_2 \\
&\quad -16p_1\sin\theta_1\Big)-24p_3p_2\sin^7\theta_2-p_3\left(\cos(2\theta_1)-5\right)^2\sin\theta_2\Big(3p_2\cos(2\theta_1)-27p_2-8p_1\sin\theta_1\Big) \\
&\quad -8p_3\sin^5\theta_2\sin\theta_1\left(3p_2\sin\theta_1-4p_1\right)-8\sin^6\theta_2\left(2p_1p_2-3\left(p_3^2-p_2^2\right)\sin\theta_1\right) \\
&\quad +16\sin^4\theta_2\sin\theta_1\left(p_1^2+6p_3^2-p_1p_2\sin\theta_1+3\left(p_3^2-p_2^2\right)\sin^2\theta_1\right)+8\sin^2\theta_2\Big(24p_1p_2+12\left(p_3^2+3p_2^2\right)\sin\theta_1 \\
&\quad +16p_1p_2\sin^2\theta_1+4\left(p_1^2+3\left(p_3^2+p_2^2\right)\right)\sin^3\theta_1+2p_1p_2\sin^4\theta_1+3\left(p_3^2-p_2^2\right)\sin^5\theta_1\Big) \\
&\quad +16\Big(16p_1p_2+8\left(p_1^2+3p_2^2\right)\sin\theta_1+20p_1p_2\sin^2\theta_1+24p_2^2\sin^3\theta_1+8p_1p_2\sin^4\theta_1 \\
&\quad +\left(p_1^2+6p_2^2\right)\sin^5\theta_1+p_1p_2\sin^6\theta_1\Big)\Big) \\
\dot{p_3} &= -\frac{\partial H_n}{\partial \theta_2} \\
&= -\frac{6\cos\theta_2}{\left(\cos(2\theta_1)+\cos(2\theta_2)-6\right)^2\left(\cos(2\theta_1)+\cos(2\theta_2)+6\right)^2}\Big(2p_2\left(\cos(2\theta_2)-5\right)\sin^3\theta_1\Big(3p_3\cos(2\theta_2)-39p_3 \\
&\quad -16p_1\sin\theta_2\Big)-24p_2p_3\sin^7\theta_1-p_2\left(\cos(2\theta_2)-5\right)^2\sin\theta_1\Big(3p_3\cos(2\theta_2)-27p_3-8p_1\sin\theta_2\Big) \\
&\quad -8p_2\sin^5\theta_1\sin\theta_2\left(3p_3\sin\theta_2-4p_1\right)-8\sin^6\theta_1\left(2p_1p_3-3\left(p_2^2-p_3^2\right)\sin\theta_2\right) \\
&\quad +16\sin^4\theta_1\sin\theta_2\left(p_1^2+6p_2^2-p_1p_3\sin\theta_2+3\left(p_2^2-p_3^2\right)\sin^2\theta_2\right)+8\sin^2\theta_1\Big(24p_1p_3+12\left(p_2^2+3p_3^2\right)\sin\theta_2 \\
&\quad +16p_1p_3\sin^2\theta_2+4\left(p_1^2+3\left(p_2^2+p_3^2\right)\right)\sin^3\theta_2+2p_1p_3\sin^4\theta_2+3\left(p_2^2-p_3^2\right)\sin^5\theta_2\Big) \\
&\quad +16\Big(16p_1p_3+8\left(p_1^2+3p_3^2\right)\sin\theta_2+20p_1p_3\sin^2\theta_2+24p_3^2\sin^3\theta_2+8p_1p_3\sin^4\theta_2 \\
&\quad +\left(p_1^2+6p_3^2\right)\sin^5\theta_2+p_1p_3\sin^6\theta_2\Big)\Big)
\end{aligned}
$$

Again the problem is isoperimetric and p_1 is a first integral.

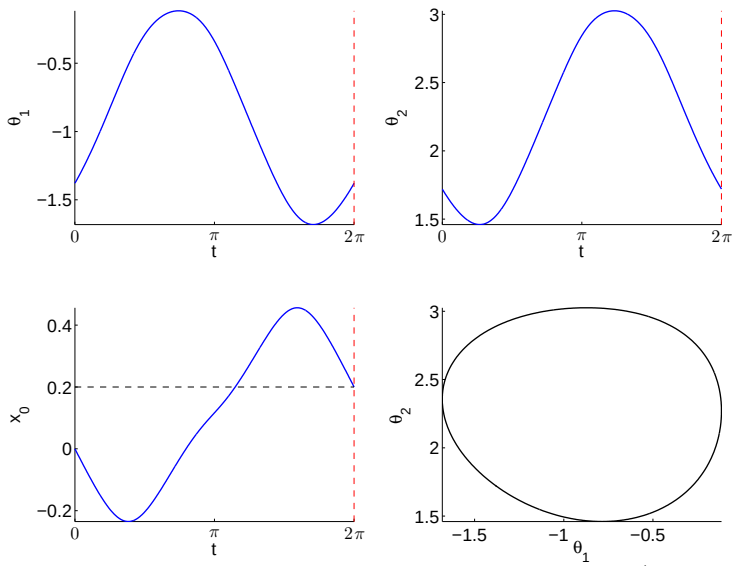


FIGURE 4. Time evolution of the state variables $q = (x_0, \theta_1, \theta_2)$ for the $\int(u_1^2 + u_2^2)$ cost.

3.3. **Numerical computations and justification of the policy of Fig.2.**

We use the Hampath code [7] at two levels

- The shooting equations associated with the problem are

$$x_0(0) = 0, \qquad x_0(2\pi) = x_f,$$
$$\theta_{1|2}(0) = \theta_{1|2}(2\pi), \qquad p_{2|3}(0) = p_{2|3}(2\pi).$$

  where for the simulations we set $x_f = 0.2$ to be compared with Fig.2.
  State variables, adjoint variables and control variables are illustrated in Fig.4-5 for the $\int(u_1^2 + u_2^2)$ cost and in Fig.6-7 for the mechanical cost.
  In Fig.8-9 and Fig.10-11, these solutions are extended to $t > 2\pi$ so that a sequence of three identical strokes are represented.
- The Hampath code is also used to show that the normal stroke is optimal testing the nonexistence of conjugate points using the variational equation to compute Jacobi fields. Recall that according to [5], given a reference curve $(q(t), p(t))$ solution in the normal case, a time $t_c \in]0, T]$ is a conjugate time if there exists a Jacobi field $\delta z = (\delta q, \delta p)$, that is a non-zero solution of the variational equation

$$\dot{\delta z}(t) = \frac{\partial \vec{H}_n}{\partial z}(q(t), p(t))\delta z(t) \tag{7}$$

  such that $\delta q(0) = \delta q(t_c) = 0$.
  We denote $\delta z_i = (\delta q_i, \delta p_i)$, $i = 1...n$, n-independent solutions of (7) with initial condition $\delta q(0) = 0$. At time t_c we have the following rank condition

$$\text{rank}\{\delta q_1(t_c), ..., \delta q_n(t_c)\} < n. \tag{8}$$

  Fig.12 (resp. Fig.13) represents the smallest singular value associated with the rank condition (8) for the $\int(u_1^2 + u_2^2)$ cost (resp. mechanical cost). We conclude the nonexistence of conjugate time for both costs.

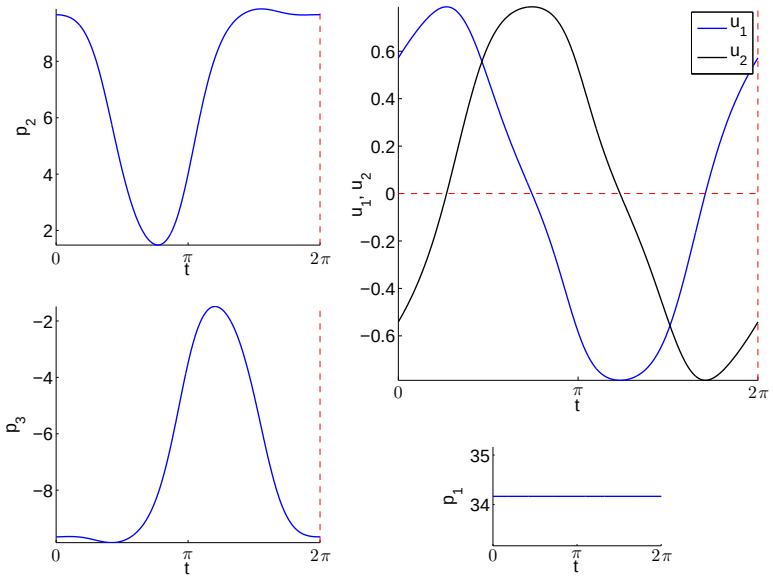


FIGURE 5. Time evolution of the adjoint variables $p = (p_1, p_2, p_3)$ and the control variables $u = (u_1, u_2)$ for the $\int (u_1^2 + u_2^2)$ cost.

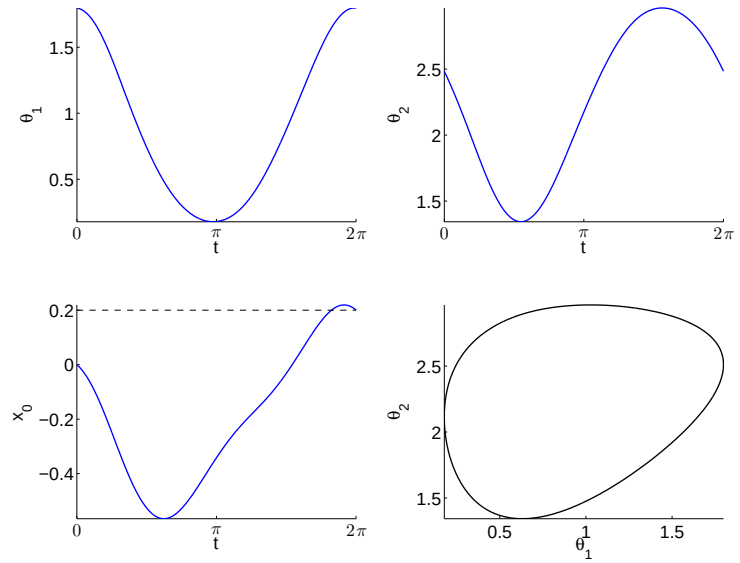


FIGURE 6. Time evolution of the state variables $q = (x_0, \theta_1, \theta_2)$ for the mechanical cost.

4. **Conclusion.**

The objective of this note is to point the interest of the copepod swimmer which can be analyzed in the framework of SR-geometry showing the accordance of the observation with simple computations concerning both normal and abnormal solutions. Further studies will allow a complete understanding in the model. A more complete analysis is based clearly on the following: understand the role of the boundary of the domain: $\theta_1 \in [0, \pi]$, $\theta_2 \in [0, \pi]$, $\theta_2 \geq \theta_1$ corresponding respectively to abnormal

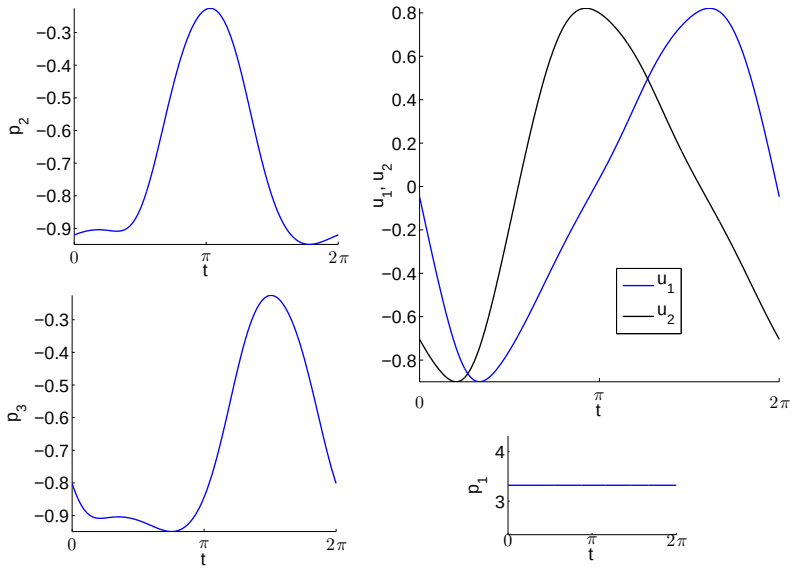


FIGURE 7. Time evolution of the adjoint variables $p = (p_1, p_2, p_3)$ and the control variables $u = (u_1, u_2)$ for the mechanical cost.

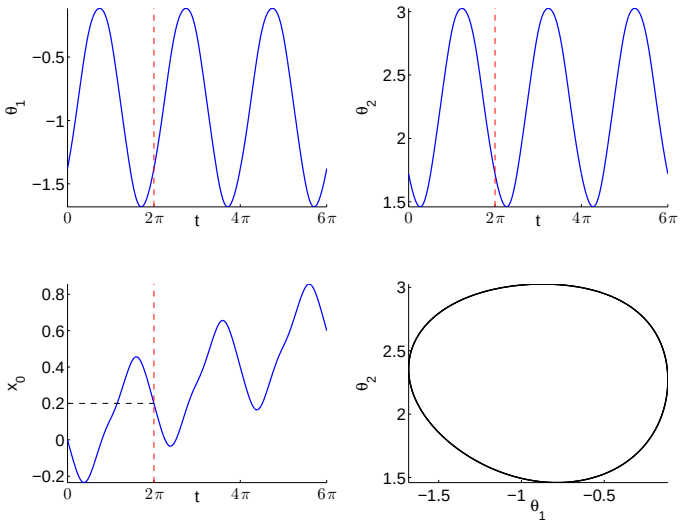


FIGURE 8. A sequence of three identical strokes for the $\int (u_1^2 + u_2^2)$ cost (state variables).

curves associated with amplitude bounds on the strokes. In particular connections between normal and abnormal curves is related to computing the optimal solutions on the bounded domain and using **the maximum principle but with state constraints**.

Complementary figures 15-20 are finally presented as a first step toward the computation of **the global solution**. They represent various stroke shapes: non self-intersecting case, the eight case and the limaçon. In all cases we have represented

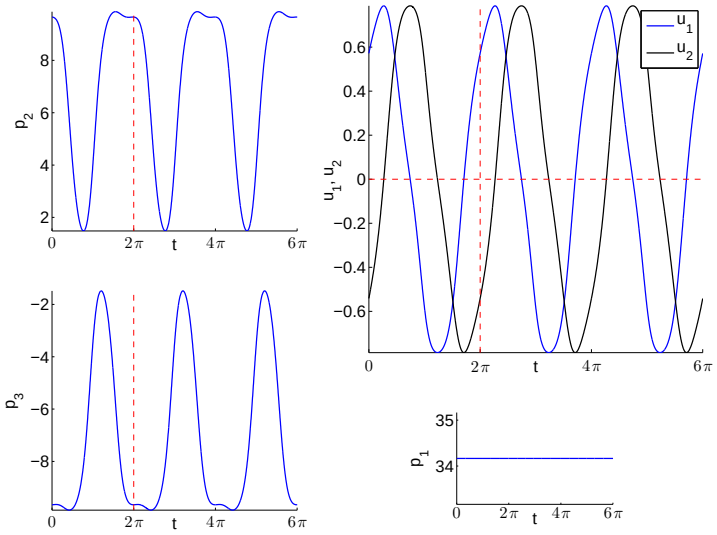


FIGURE 9. A sequence of three identical strokes for the $\int(u_1^2+u_2^2)$ cost (adjoint variables and control variables).

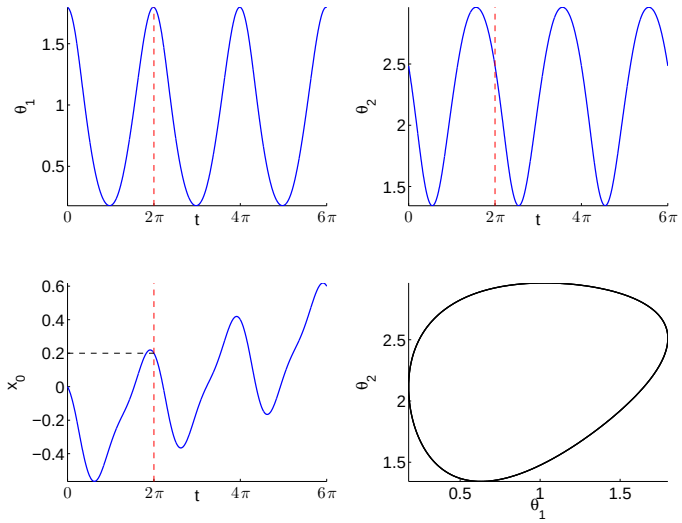


FIGURE 10. A sequence of three identical strokes for the mechanical cost (state variables).

conjugate point location on a stroke (if existing) and *the energy level* corresponding to the value function of the stroke. See also Fig.17 for more self intersection.

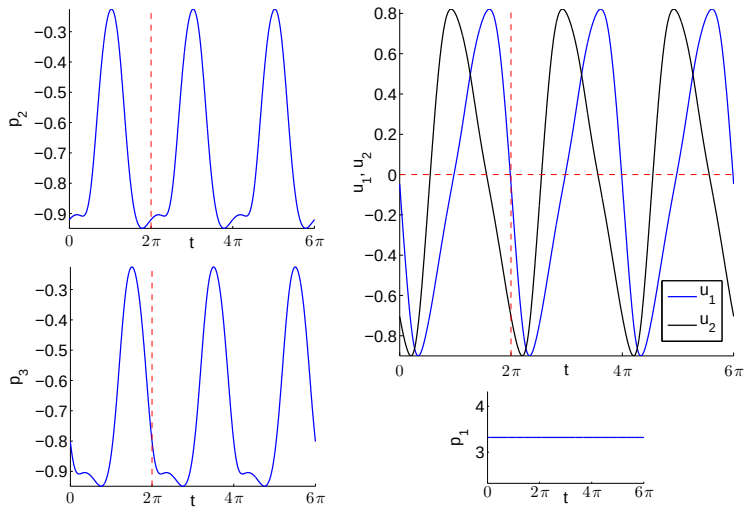


FIGURE 11. A sequence of three identical strokes for the mechanical cost (adjoint variables and control variables).

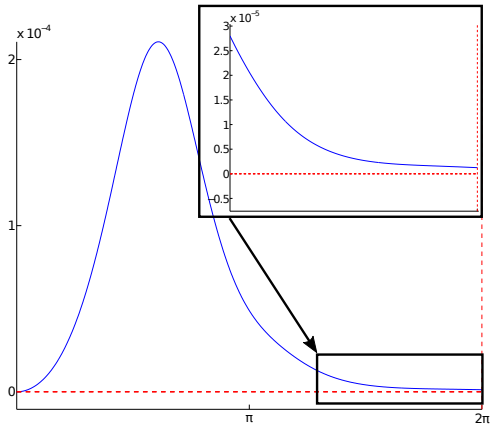


FIGURE 12. Second order sufficient condition checked on a stroke for the $\int(u_1^2 + u_2^2)$ cost. The smallest singular value associated with the rank condition (8) doesn't vanish on $]0, 2\pi]$, and there is no conjugate time.

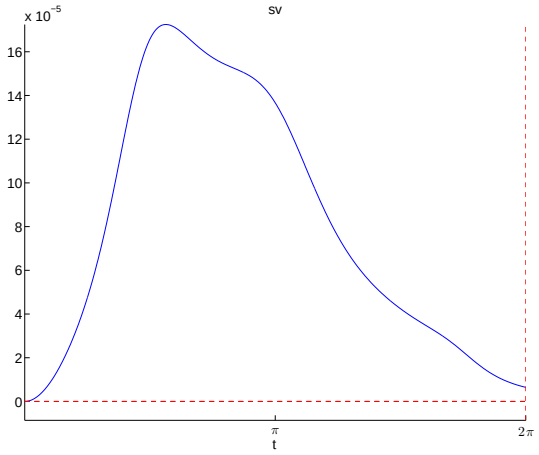


FIGURE 13. Second order sufficient condition checked on a stroke for the mechanical cost. The smallest singular value associated with the rank condition (8) doesn't vanish on $]0, 2\pi]$, and there is no conjugate time.

REFERENCES

[1] F. Alouges, A. DeSimone, L. Giraldi and M. Zoppello. *Self-propulsion of slender microswimmers by curvature control: N-link swimmers.* Int. J. Nonlinear Mech., **56** (2013).

[2] F. Alouges, A. DeSimone, A. Lefebvre. *Swimming at low Reynolds number at optimal strokes: An example.* J. of Nonlinear Sci., **18** (2008), no. 3, 277–302.

[3] L.E. Becker, S. A. Koehler and H.A. Stone. *On self-propulsion of micro-machines at low Reynolds number: Purcell's three-link swimmer.* Journal of Fluid Mechanics, **490** (2003), 15–35.

[4] P. Bettiol, B. Bonnard, L. Giraldi, P. Martinon and J. Rouot. *The three links Purcell swimmer and some geometric problems related to periodic optimal controls.* Submitted (2015).

[5] B. Bonnard and M. Chyba. *Singular trajectories and their role in control theory.* Mathématiques & Applications (Berlin), **40**. Springer-Verlag, Berlin (2003), 357 p.

[6] T. Chambrion, L. Giraldi and A. Munnier. *Optimal strokes for driftless swimmers: A general geometric approach.* Submitted (2014).

[7] O. Cots. *Contrôle optimal géométrique : méthodes homotopiques et applications.* Phd thesis, Institut Mathématiques de Bourgogne, Dijon, France (2012).

[8] L. Giraldi, P. Martinon and M. Zoppello. *Optimal design of the three-link Purcell swimmer.* Phys. Rev. E, **91** (2015).

[9] R. Montgomery. *A tour of subriemannian geometries, their geodesics and applications.* American Mathematical Society, Providence, RI. **91** (2002), 259 p.

[10] E. Passov and Y. Or. *Supplementary document to the paper: Dynamics of Purcell's three-link microswimmer with a passive elastic tail".* Supplementary Notes.

[11] E. M. Purcell. *Life at low Reynolds number.* Am. J. Phys. **45** (1977), 3–11.

[12] D. Takagi. *Swimming with stiff legs at low Reynolds number.* Submitted (2015).

[13] D. Tam and A.E. Hosoi. *Optimal Stroke Patterns for Purcell Three-Link Swimmer.* Phys. Rev. Lett. **98** (2007).

[14] G.I. Taylor. *Analysis of the swimming of microscopic organisms.* Proc. Roy. Soc. London. Ser. A. **209** (1951), 447–461.

[15] M. Zhitomirskiĭ. *Typical singularities of differential* 1*-forms and Pfaffian equations.* American Mathematical Society, Providence, RI. **113** (1992), 176 p.

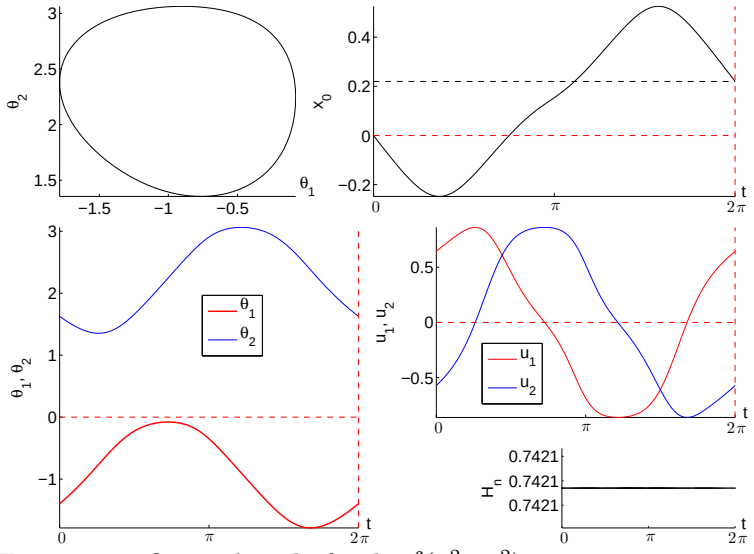


FIGURE 14. Optimal stroke for the $\int(u_1^2+u_2^2)$ cost:non intersecting case. We fixed the displacement to $x_0(2\pi) = 0.22$.

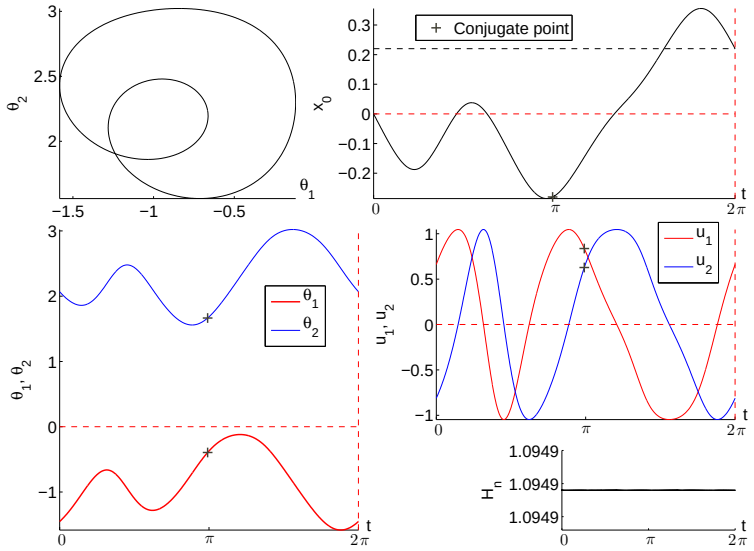


FIGURE 15. Optimal stroke for the $\int(u_1^2 + u_2^2)$ cost:limaçon with inner loop. We fixed the displacement to $x_0(2\pi) = 0.22$.

E-mail address: bernard.bonnard@u-bourgogne.fr
E-mail address: mchyba@math.hawaii.edu
E-mail address: jeremy.rouot@inria.fr
E-mail address: dtakagi@hawaii.edu
E-mail address: rzhou@hawaii.edu

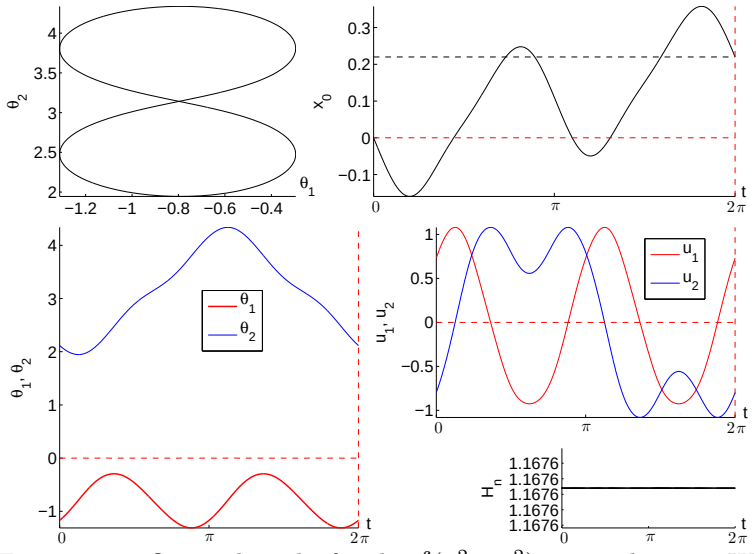


FIGURE 16. Optimal stroke for the $\int(u_1^2+u_2^2)$ cost:eight case. We fixed the displacement to $x_0(2\pi)=0.22$.

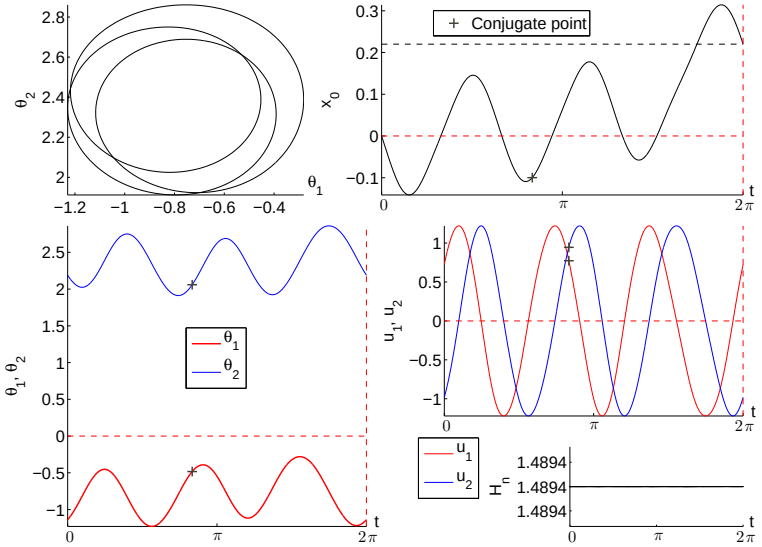


FIGURE 17. Optimal stroke for the $\int(u_1^2+u_2^2)$ cost:multiple self intersections. We fixed the displacement to $x_0(2\pi)=0.22$.

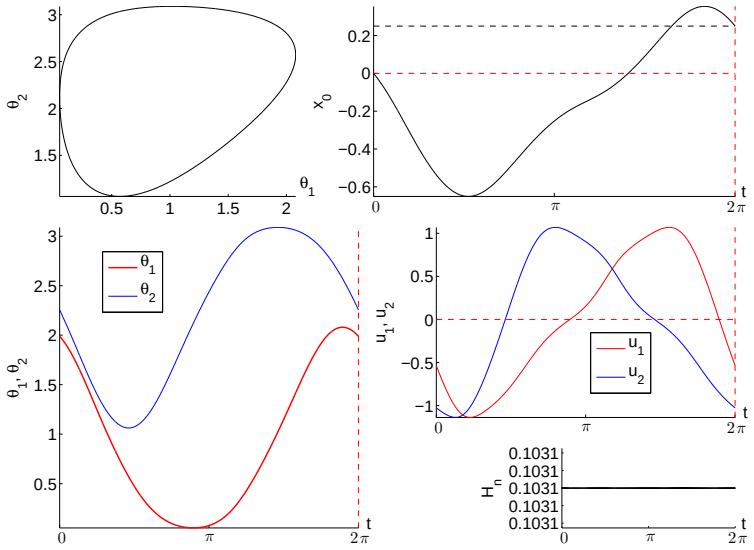


FIGURE 18. Optimal stroke for the mechanical cost:non intersecting case. We fixed the displacement to $x_0(2\pi) = 0.25$.

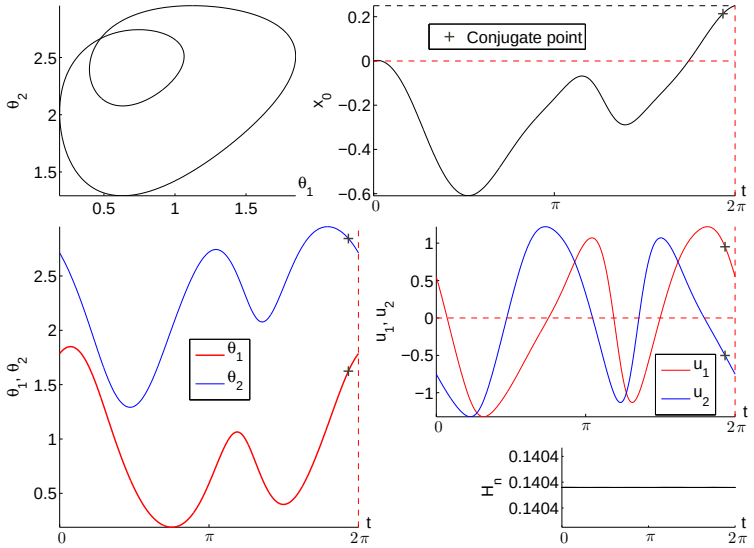


FIGURE 19. Optimal stroke for the mechanical cost:limaçon with inner loop case. We fixed the displacement to $x_0(2\pi) = 0.25$.

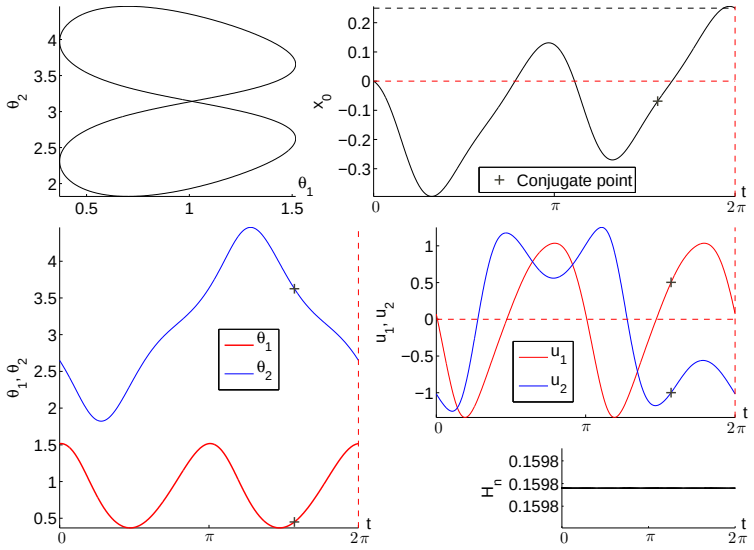


FIGURE 20. Optimal stroke for the mechanical cost:eight case. We fixed the displacement to $x_0(2\pi) = 0.25$.